LANSCE H+ CVD Diamond Target Test

Tarik Saleh

Abstract

This experiment investigated using a chemical vapor deposition (CVD) grown diamond as a beamstop for a 2.5MeV proton beam for eventual use as a chopper target in the front end of the Spallation Neutron Source (SNS). Diamond has excellent strength and thermal properties for a beamstop, but is susceptible to radiation damage and subsequent graphitization. Some experiments have shown that diamond can anneal at higher temperatures prolonging its use under radiation. A diamond beam stop was fabricated and tested at LANL. The diamond was placed under similar implantation conditions as it would experience in use, 10^{21}/protons/day/cm^2. Two experiments were run with distinct diamond targets. The first failed in 4.5 minutes, the second in 29 minutes. Diamond does not appear to self anneal fast enough under the implantation and temperature conditions in the SNS. It is not a suitable material for this beamstop.

Introduction

Lawrence Berkeley National Laboratory is building the Front End of the Spallation Neutron Source(SNS). The Medium Energy Beam Transport (MEBT), in the SNS Front End, contains a beam chopping target that must withstand H- ion beam pulses with peak power densities of approximately 400 kW/cm^2. The high thermal conductivity and mechanical strength of chemical vapor deposition (CVD) grown diamond put it at the top of a short list of viable candidate materials for this target. Experimental results have shown, however, that damage induced in CVD diamond by hydrogen-ion implantation and/or radiation can cause degradation of its thermal conductivity and ultimate strength. Experiments have also shown that, in some cases, such damage can be repaired through annealing.

Literature values for the damage threshold are between 10^{17} and 10^{20} protons/cm^2. The primary damage mechanism is the displacement of carbon atoms off of their lattice sites and into interstitial positions by the impinging protons. The damage causes the formation of graphite and amorphous carbon, which degrades the strength and conductivity of the diamond, which could cause a structural failure of the beam stop.

At higher temperatures the displaced carbon atoms become more mobile and will migrate back to their proper lattice positions. The onset of increased mobility of the displaced carbon atoms occurs around 400°C. The hypothesis of the experiment was that the temperature increase caused by the incident beam would increase the mobility of the displaced carbon atoms. This would, in effect, heal the damage as it was caused. The ideal end would be a target that operated at a temperature that allowed the diamond to heal itself so that the total damage (# of i-V pairs at any one time) remains below the damage threshold.

There is a large amount of work but little concrete consensus on healing radiation damaged diamonds. The damage criteria, annealing temperatures and graphetiztion temperatures vary quite a bit from paper to paper. Because of this there was a large degree of uncertainty of success.

Los Alamos National Laboratory (LANL) has a proton beam at the Los Alamos Neutron Science Center (LANSCE). A LANSCE copper beam stop was modified to hold sample targets and installed in a diagnostic beam box in the LANSCE H- injector. The target area of the beam stop consisted of CVD diamond brazed to molybdenum brazed to a water-cooled copper block. The geometry of the target was designed such that the diamond would reach thermal equilibrium at a temperature within its “healing” range.

The target was subjected to a proton beam designed to test if the diamond would anneal under implantation and temperature conditions similar to those of the SNS.

Background

Diamond consists of carbon atoms bonded in sp3 tetrahedrons. The 4 valence electrons are all involved in the tetrahedral bonding. There are no free electrons for electrical conduction in an undoped diamond. Due to the carbon atom's small size, there is a high density of tightly bonded nuclei in the diamond structure. The combination of sp^3 bonding and small atomic size lead to excellent strength, high thermal conductivity and a very low coefficient of thermal expansion.

The high strength and thermal conductivity of diamond make it an ideal candidate for use as a beam stop. The thermal conductivity of CVD diamond ranges between 1200-2400 W/mK , 3-6 times that of copper.

Generally, CVD grown diamond is a polycrystal grown from a chemical reaction involving gasses that deposit diamond on a metal substrate. The diamond tends to grow in columnar grains (the columns in the direction of growth). After growth the diamond is laser cut to shape and ground and polished to remove the topography on the growth face. The quality of CVD diamond can vary quite widely. The very best samples can have thermal and optical properties similar to natural type IIa diamond. Young's modulus for CVD diamond is similar to natural diamond, but the rupture and yield strengths are often half that of natural diamond. Fracture toughness is usually higher in CVD diamond, due to the presence of grain boundaries, which impede crack growth. [Sussman]

The specific diamond used in this experiment was a CVD grown, undoped, polycrystalline diamond. It appeared black and slightly translucent. The coloration comes from many twin defects and a high dislocation density as well as sp^2 bonded carbon on the grain boundaries. The diamond was grown from a mixture of methane, hydrogen and argon gas and deposited on a molybdenum substrate held between 800 and 900°C. The diamond was obtained from Crystalline Manufacturing Limited.

Radiation damage

Due to their low mass, carbon atoms are susceptible to displacement when irradiated with accelerated particles. The most common displacement phenomenon is the displaced atom going to an interstitial site coupled with a vacancy forming on the original site (i-V pairs). Additionally, an incident proton will occasionally cause larger damaged regions.

As temperature increases, the interstitial atoms will become more mobile and will cause the i-V pairs to recombine. The temperature where mobility begins is given as roughly 400-600°C. [Palmer] This annealing is thought to be able to cure radiation damage up to a critical level of implantation, beyond which the structure is too damaged to be annealed. The critical level of implantation is somewhat ambiguous. Implantation level is given alternately as an absolute number of implantations/cm^2 (total incident ions) or as a number of permanent damaging implantations (total incident ions minus number of healed sites during implantation). The absolute number is temperature independent, while the other is temperature sensitive, varying as the rate of recombination changes with temperature. This said, using data garnered from neutron and other ion implantation experiments, it appears that permanent damage occurs in the range between 10^{17} and 10^{20} implantations/cm^2. [Vandersande, Kalish]

Rate & Threshold

As the amount of proton implantation increases, the properties of the diamond begin to change. Critical to this experiment is the degradation in thermal conductivity. As the thermal conductivity is decreased, the advantages of using diamond are nullified. Additionally, at a certain level of damage, the carbon atoms will form amorphous regions and then, at higher temperatures and levels of damage, graphite regions.

As implantation and damage increase the thermal conductivity of diamond will decrease. On tests on natural single crystal diamond irradiated by neutrons, thermal conductivity at room temperature was seen to

drop by an order of magnitude between unirradiated diamonds and diamond irradiated with $3x10^{16}$ n/cm2. The thermal conductivity dropped another order of magnitude between diamonds irradiated $3x10^{16}$ and $6x10^{17}$ neutrons/cm^2. [Vandersande]

However, after amorphisation and graphitization occur, the conductivity in that small area will drop drastically causing dramatic surface heating. The level of proton implantation in CVD diamond needed to start amorphisation is unclear. However, Vandersande shows amorphisation in neutron irradiated samples of natural diamond to begin at 10^{20} neutrons/cm^2.

Further complicating the issue is that there is a natural temperature at which diamond begins to graphitize in a vacuum and in air. For natural diamond this is given as 900K in air, for surface oxidization and 1800K in an inert atmosphere. The combination of elevated temperature and radiation damage may increase the rate of amorphisation where damage levels are high enough, however, the literature does not clearly quantify these phenomena.

Undoped diamond has an extremely low electrical conductivity. However graphite has high conductivity. Any surface amorphisation and graphitization should be detectable with an ohmmeter.

Experiment

Target

The beam stop was fabricated out of a previously used LANSCE beam stop. The stainless steel to copper brazement and the cooling channels were already in place, as were the connections to the beam stop column. The beam stop originally consisted of a 2.5 x 8.2 x 1.9 cm block of stainless steel brazed on top of a 5.75 x 8.2 x 1.9 cm block of copper. A thermal isolation channel was milled from the front face of the target. Three recesses were also milled from the target's face to hold the diamond/molybdenum brazed assemblies. These recesses were placed so that when the beam stop was rotated 30°, the diamonds would be on beam center. Two diamond wafers, 10x15x0.5 mm, were brazed to an "L" shaped molybdenum thermal well. See figure 1 for photograph and appendix A for dimensions and details.

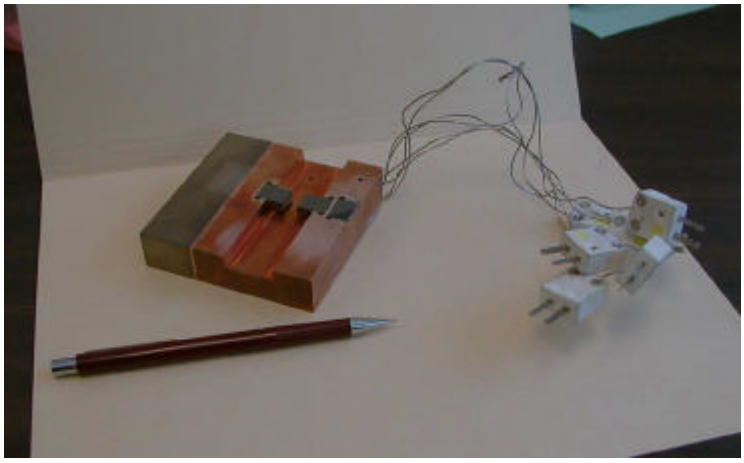

Figure 1 Beamstop

The diamond was brazed to the molybdenum with Cusil ABA braze material. Cusil ABA has a composition of 63% Cu, 35.25% Ag, 1.75% Ti, it has a solidus at 780°C and a liquidis of 815°C. The molybdenum was brazed to the copper using Incusil ABA. Incusil ABA has a composition of 59% Cu, 27.5% Ag, 12.5% In and 1.25% Ti, it has a solidus of 605°C and a liquidus of 715°C. Both brazes were done in a vacuum furnace under a partial pressure of argon.

Six thermocouple holes were drilled through the back of the copper target. Four of the six holes were drilled into the molybdenum thermal wells to a point 1mm below the diamond's surface. The upper diamond was monitored by thermocouples 1, 2 and 3. Number one monitored bulk copper temperature above the upper diamond and numbers 2 and 3 monitored temperature in molybdenum 1mm below the diamond. Thermocouple numbers 4, 5 and 6, corresponding to bulk copper temperature and two molybdenum temperatures respectively, monitored the temperatures near the lower diamond.

A thermocouple feed-through was fabricated to allow the thermocouple leads to pass from the vacuum to the outside of the beam box.

A fixture, shutter and sapphire window were fabricated so that an optical pyrometer could be used to monitor the surface temperature of the diamond while the beam was on. Unfortunately the pyrometer could not be focused correctly in use on the actual beam box. No data was recorded from the pyrometer. The design can be seen in Appendix B.

Beam Conditions

At the time of the test the SNS beam conditions were as seen in Table 1. In designing the initial test a higher proton implantation rate and a lower power density were chosen. The lower power was to keep the temperature excursions as low as possible. An ideal experiment would maintain a high average temperature within the annealing range. However, due to the pulsed nature of the beam, a lower average temperature was chosen so that the peak temperature exposures would not exceed the graphitization temperature of the diamond (see FEA section for predicted temperatures). The higher implantation rate was to keep the experiment running at a faster rate, so changes could be observed over the course of days and weeks, rather than months. The initial LANSCE beam conditions for the first and second test can be seen in Table 1.

	SNS		LANSCE1	LANSCE 2
Peak Current =	56	mA	20	20
Energy =	2.5	MeV	0.75	0.75
Frequency =	60	Hz	120	15
Duty Factor	0.36	%	1.8	0.225
σx =	0.383	cm	0.12	0.12
σy =	0.161	cm	0.12	0.12
Avg Target power =	499.41	W	270.0	33.750
Protons/sec/cm^2 =	4.25366E+15	#/sec/cm^2	2.84E+16	3.55349E+15

Table 1

Beam implantation density was calculated by assuming a Gaussian profile and placing 66% of the power across an ellipsoidal area with diameters σx and σy. This is where implantation density was highest and most relevant to the experiment. The actual beam profile for the two tests was back calculated from an emittance scan downstream of the target. The results can be seen in appendix C.

Finite Element Analysis

The dimensions of the target and thermal well were optimized by finite element analysis (FEA). The dimensions were designed such that under the LANSCE beam, the average temperature would be within the self-healing range for diamond, while the peak temperature due to the millisecond scale bursts of power would be below graphitization temperature. This analysis was done by modeling an average power input and by modeling a time dependent input of actual power at the millisecond scale.

Two ANSYS analyses were performed to simulate the 2 tests run at LANSCE. The 270W experiment yielded a theoretical maximum surface temperature of 1080°C and a temperature at the thermocouples (1mm below diamond surface) of 424°C. The 37.5 W case predicted a maximum surface temperature of 113°C and a thermocouple temperature of 76°C. The model was based on applying an average power across the total beam spot (6σ) to reach a steady state and then applying a Gaussian beam in a 150 microsecond pulse. The maximum temperature is achieved at the end of this pulse, and then the model is allowed to cool for 8.18 milliseconds. The temperature spike from the initial pulse completely disappears at the end of the cooling period. Analyses for the steady state, temperature spikes and cooling can be found in appendix D

Test Conditions

The first test was run in two phases. The first 15 seconds were run at frequency of 30Hz, 20ma current with a $150x10^{-6}$ sec gate time. The average power during this time was 67.5 W and there were approximately $1x10^{17}$ protons implanted per cm^2 area. The second part of the test was run at 120Hz frequency, 20 ma current and a $150x10^{-6}$ sec gate time for 205 seconds. Total protons implanted between the two phases were $5.9x10^{18}$. The experiment was halted after small piece of diamond (approximately 1x2mm) was observed to have suddenly fallen off the surface.

The second test was run at 15 Hz, 20 ma with a $150x10^{-6}$ gate time for 26 minutes 30 seconds. Average power was 33.7 W. The total number of protons implanted was approximately $5.6x10^{19}$/cm2. The experiment was halted shortly after the diamond in the center of the beam spot was observed to be glowing and sparking. Thermocouple #2, one of the ones just below the target, broke when the leads were switched between the lower and upper target. However this thermocouple was somewhat redundant being spaced only 1 mm away from thermocouple #3.

Results

Experiment #1

The temperature profile for the first experiment can be seen in Figure 2. In the first part, the two thermocouples just below the diamond target (thermocouples 2 & 3) reached a maximum temperature of approximately 114°C. The data sampling rate was in 10 second intervals over a 15 second experiment and it is difficult to report the maximum temperature accurately. The second part of the first experiment yielded a peak temperature of 484°C on thermocouple 2, 468°C on thermocouple 3 and 41.3°C on thermocouple #1. The thermocouples below the target (2&3) jumped from room temperature to above 400°C within the first 20 seconds of the experiment.

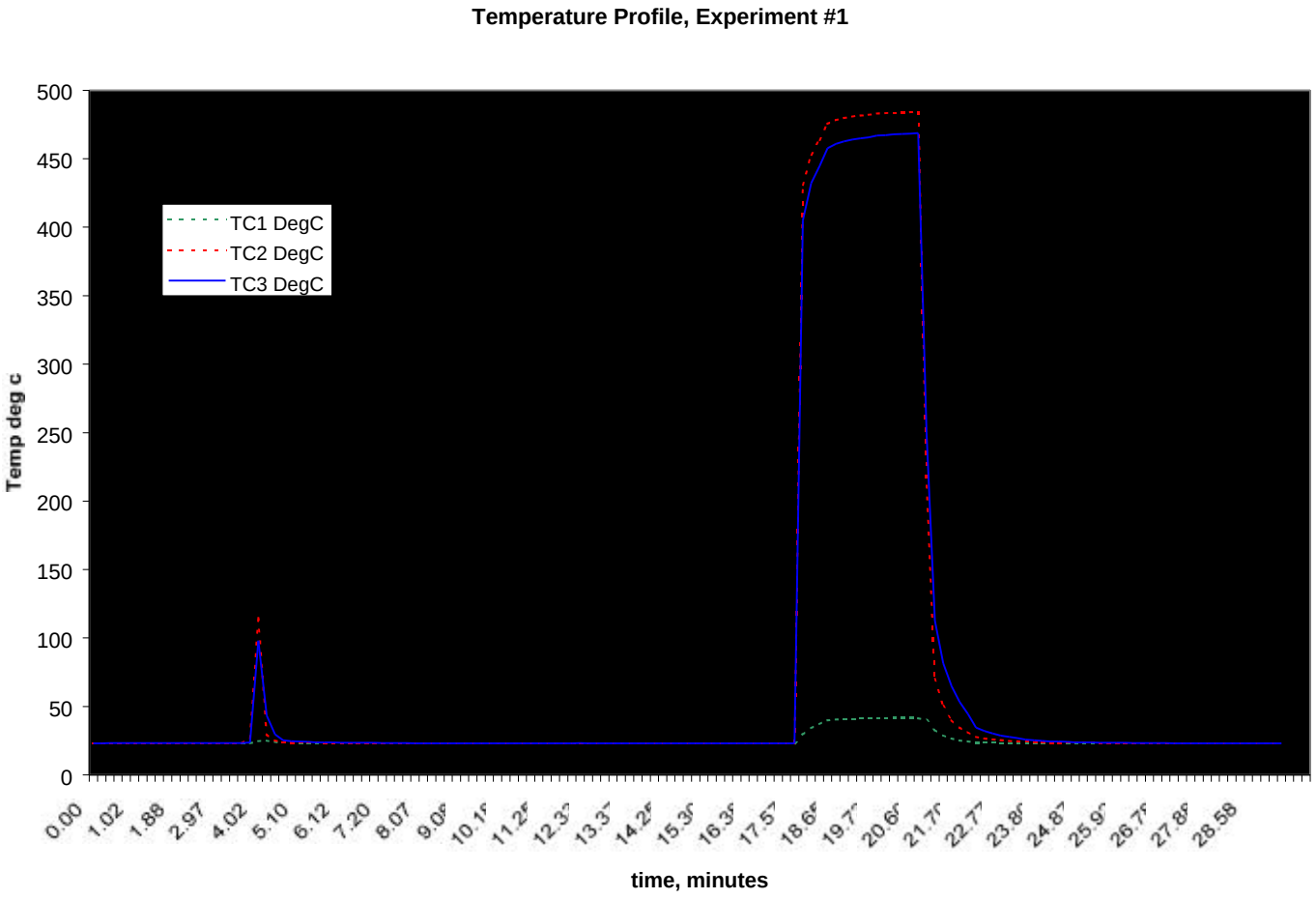

Figure 2

Upon turning on the beam, the beam spot immediately began glowing blue. The beam spot appeared to be 7 mm in diameter with a 1mm "tail" off of the left side of the beam. During the first part of the experiment, the beam spot stayed completely blue. During the second part of the experiment the beam spot started off the same blue color. Over the first minute the center of the beam slowly faded to a whitish-blue color. The outer mm of the beam spot retained its blue color. At two minutes the core of the beam spot had turned to a whitish red and the very center of the beam began glowing with an intense white light. Sparks began emitting from center of the beam spot shortly after 2 minutes. Over the next minute and a half, small glowing regions began appearing around the center of the beam, slightly offset to the right side. Sparks were emitted from all the glowing spots. The sparks were coming from a 2x1 mm area to the right and above the center of the beam spot. At 3 minutes and 25 seconds a 2x1 mm section of the diamond started glowing suddenly and then fell off from below and to the right of the beam spot. The beam was shut off immediately after this occurred. See figure 3.

Figure 3

Experiment #2

The temperature profile for the second experiment on the upper diamond can be seen in figure 4. The data sampling rate was every second for the first 13 minutes and every 10 seconds after that. Thermocouple #3 (just below the target) reached a maximum temperature of 64.9°C. The temperature on thermocouple 3 jumped from room temperature to just over 60°C within the first 10 seconds of the experiment. Thermocouple #1 reached a maximum of 24.5°C during the experiment.

Upon turning on the beam, the beam spot immediately began to glow a uniform orange color. The beam spot was round with a 7mm diameter. By 1:30 into the experiment the beam spot appeared blue in the center with an approximately 1mm orange halo. At 4:30 the center of the beam had faded to light blue while the halo had split into an orange outer ring and a blue inner ring that was half the size of the outer. By 7:00 the center part of the beam spot had faded to white and a very faint glowing white spot appeared in the beam center. At 14 minutes, the orange halo had disappeared; it gave way to blue. The center was still white and there was still a glowing speck in the center. By 16:30 the center glowing speck was more distinct. At 25:30 the center began glowing distinguishably and shortly after sparking began to occur. (Figure 5) After the beam stop was removed from the chamber and visually inspected, a very faint ring was noted on the surface. The ring was approximately 7mm diameter and was centered on the damaged region of the diamond. It corresponds fairly well with the beam spot.

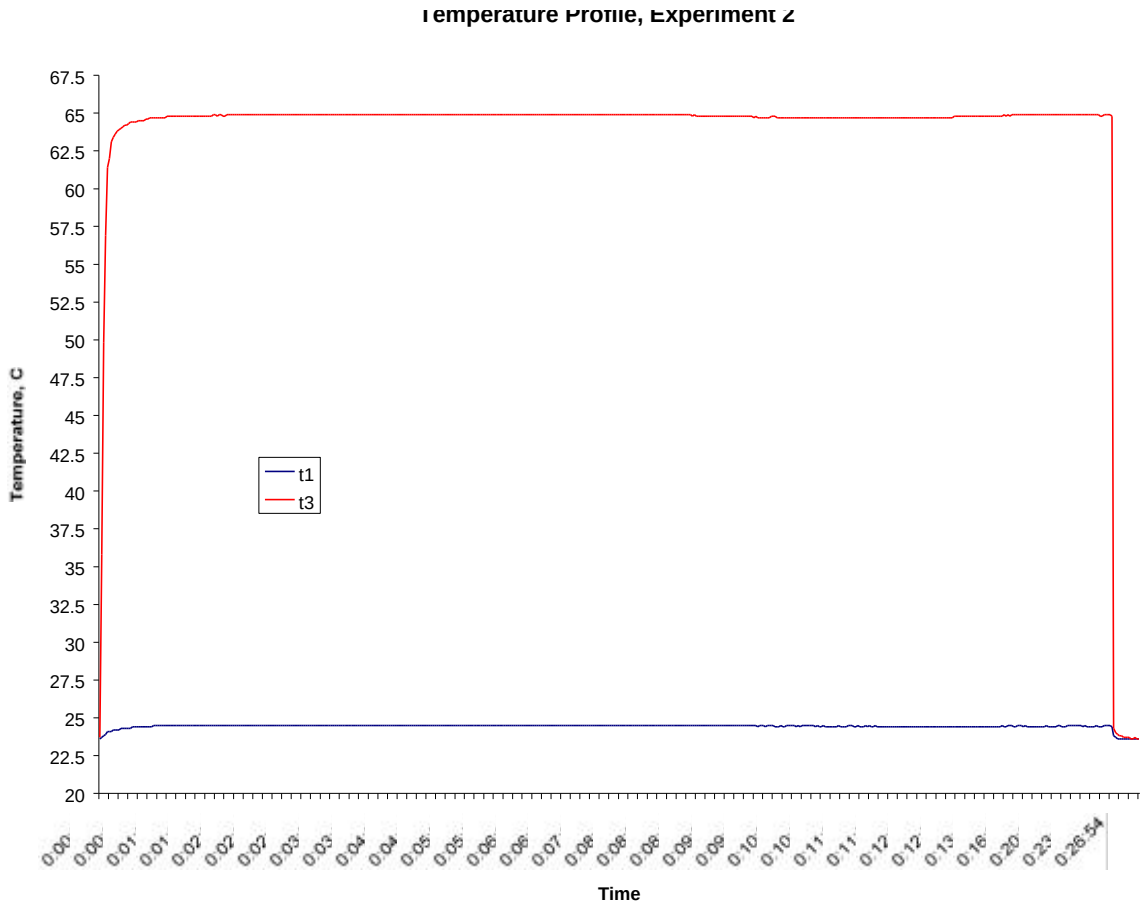

Figure 4

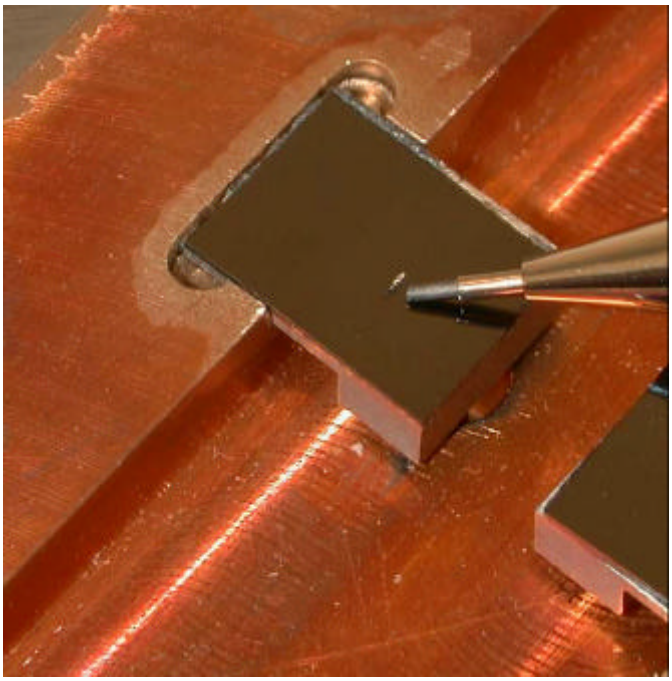

Figure 5, top diamond with .7mm graphite pencil

Resistance

A simple ohmmeter was used to test the surface resistance of the diamonds before and after the experiment. Before the experiment, both diamonds registered as an open circuit (Extremely high resistance). After the experiment (experiment #1) the lower diamond registered as an open circuit across the unbroken surface. However, the two broken regions registered a resistance when the probes were placed within each broken region. There also was an electrical path noted between the two regions when the one probe was placed within one break and the other probe within the opposite break. The resistance was approximately 10 MΩ. The upper diamond, experiment #2, registered a resistance of approximately 20MΩ everywhere inside the ring on the surface. No conductivity was registered outside of the ring.

Discussion

Experiment #1

During the first experiment the first definitive sign of damage, bright glowing in the center of the beam spot, occurred after two minutes into the higher power part of the experiment. The amount of implantation at this point was $3.5x10^{18}/cm^2$. At one minute when the center of the beam spot was fairly white the number of implantations was $1.8x10^{18}$. The temperature range measured by the thermocouples was as predicted.

There were two likely conclusions based on these results. The first was that the diamond was unable to heal itself under the temperature and implantation conditions, amorphous carbon and/or graphite formed and these non-diamond regions heated up until they glowed and sparked and broke off the diamond surface. The second possibility was that due to the underlying topography of the surface and impurities and grains of the diamond, regions of the diamond mechanically fatigued off the surface or were thermally isolated and then heated up and fatigued off.

Figure 6 shows an optical micrograph of one of the fractured surfaces of the lower diamond. The magnification is 100 times. The crack surface is made of concentric rings from the surface down to the bottom of the crack. This supports a failure based on a crack progressing over multiple temperature cycles. Presumably the cracks started with the onset of graphitization and the subsequent strength loss. With each temperature cycle the beam spot expanded and cracked further into the diamond surface. Figure 7 shows the same phenomena for the fracture region in the upper diamond used in experiment 2.

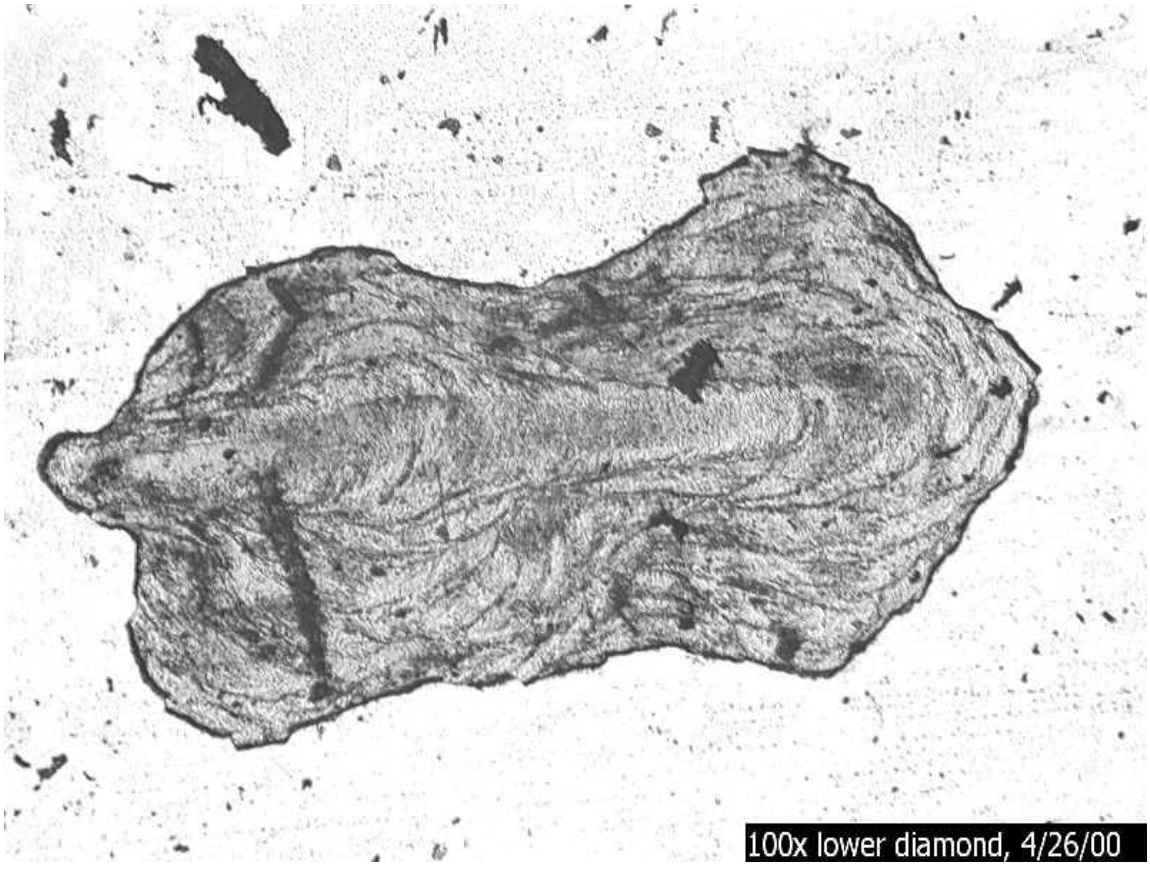

Figure 6 lower diamond fracture region

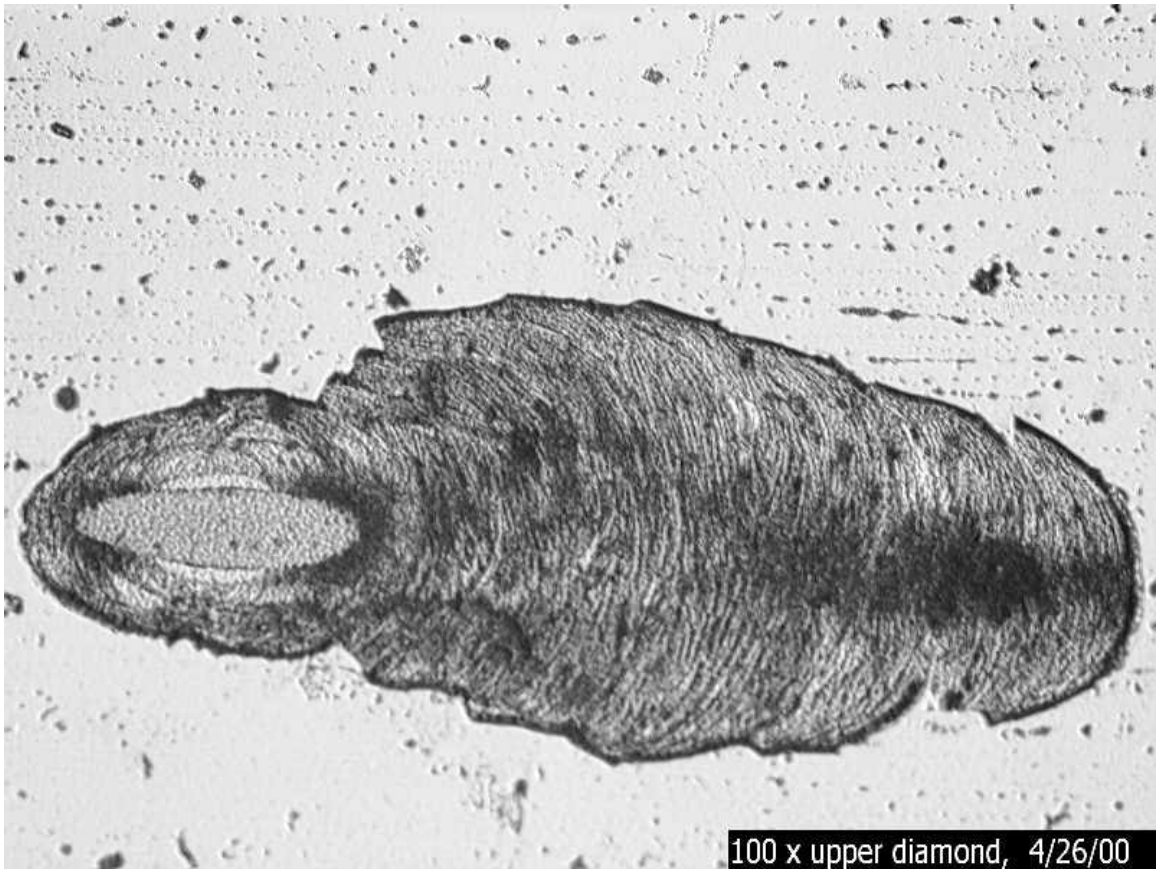

Figure 7 upper diamond fracture region

Experiment #2

This experiment was designed to test the hypothesis about the results of the first experiment. The same amount of power/pulse was kept, however the number of pulses/second were reduced by a factor of 8. This also reduced the implantation density by a factor of 8. The lower average power should have removed the likelihood of the diamond failing by fatigue or thermal isolation. However, if implantation damage and subsequent amorphisation or graphitization occurred, the glowing spots should have been repeated, only this time after a longer period of irradiation.

As it occurred, the same mechanism of failure occurred after 26:30 of irradiation.

At 8:30 into the experiment, when the first evidence of bright glowing occurred, hence amorphisation or graphitization, there were approximately 1.8×10^{18} protons/cm^2. At 4:30 where the center began to turn white, there were approximately 2.5×10^{17} protons/cm^2. The bulk temperature in the diamond scaled appropriately to that of the first experiment and the initial FEA modeling.

Since the temperature was so low in the second experiment, annealing should not have occurred. This is consistent with the fact that we saw similar phenomena in both experiments, but at lower implantation density in the second. Suggesting that the first experiment experienced some annealing while the second did not.

The fact that there is a conductive region over most of the beam spot on the upper diamond indicates that the implantation caused surface damage in the form of graphitization over most of the beam spot.

While there is non-conclusive evidence that some annealing occurred during the first test, it was a fairly inconsequential amount. In use at a higher power density such as seen in the SNS, it is doubtful that the bulk temperature could be held high enough to cause both rapid healing and avoid having the temperature spikes graphitize the diamond. Even if these criteria were met, it appears that the rate of annealing would be far too small to allow the SNS target to operate for a month without failure.

Future Research

While the diamond was shown to be an inappropriate material for a beam stop used in a pulsed SNS type proton beam, the theory of a self healing diamond beam stop may be viable under different conditions. The success of using a diamond beam stop in this experiment was limited by the nature of the radiation input. The pulsed beam and its large power densities on the millisecond scale caused large temperature excursions from the bulk temperature in the diamond. Because of this, the bulk temperature in the diamond needed to be kept low so that the temperature excursions did not reach graphitization temperatures. While the bulk temperature was in the 450°C range, theoretically above the temperature at which the Frenkel pairs became mobile, it was at the low end of the mobility temperature range. With a constant beam, the diamond could be held at a much higher bulk temperature. This approach would avoid the temperature spikes into the graphitization range and would increase the mobility of the carbon atoms.

An optimum experiment would have an implantation rate just above the damage limit and a constant beam. For example, a beam that inputs $5x10^{17}$ protons/day/cm^2 with a power density and target design that keeps the target at a constant 700-800°C. This would show, over the course of two or three days, whether or not a diamond could self heal. With appropriate surface monitoring, the steady state temperature would start to grow in spots or over a larger area if amorphisation or graphitization occurs. However, a successfully healing target could stay viable for well over the 5 hours it would take to reach $1x10^{17}$ protons/cm^2. If the test could be made to run successfully at this damage rate, higher rates could be tried. Perhaps some insight to the behavior of the diamond could be made that would be applicable to using diamond as a beam stop under more realistic use conditions.

The key to future experiments would be to obtain a very accurate measurement of the surface temperature. An infrared camera or a more carefully aligned and calibrated pyrometer would suffice.

Conclusion

CVD diamond was proposed as a material which might be able to withstand the high power density of the SNS pulsed proton beam. The material properties of diamond were ideal for the purpose except for the tendency of diamond to sustain radiation damage under incident protons. The literature existing on the subject, while vague, suggested that there was a possibility diamond might be able to self anneal under the heat of a proton beam. If the rate of self healing was high enough the diamond might be able to endure the SNS proton beam for a month. Two experiments were carried out at the LANSCE facility, the first under similar conditions to the SNS beam, the second under 8 times lower power and at a lower temperature. Both experiments ended in small sections of the target glowing, sparking and chipping off. The results of the first experiment suggested that the diamond would be damaged far faster than it could self anneal under realistic temperature constraints. The second experiment showed that the failure mechanism in the first experiment was due to radiation damage, not due to defective diamonds. CVD diamond appears incapable of meeting the extended performance requirements of the SNS beam. Other target materials and configurations will be explored.

Appendix A

Beamstop Layout

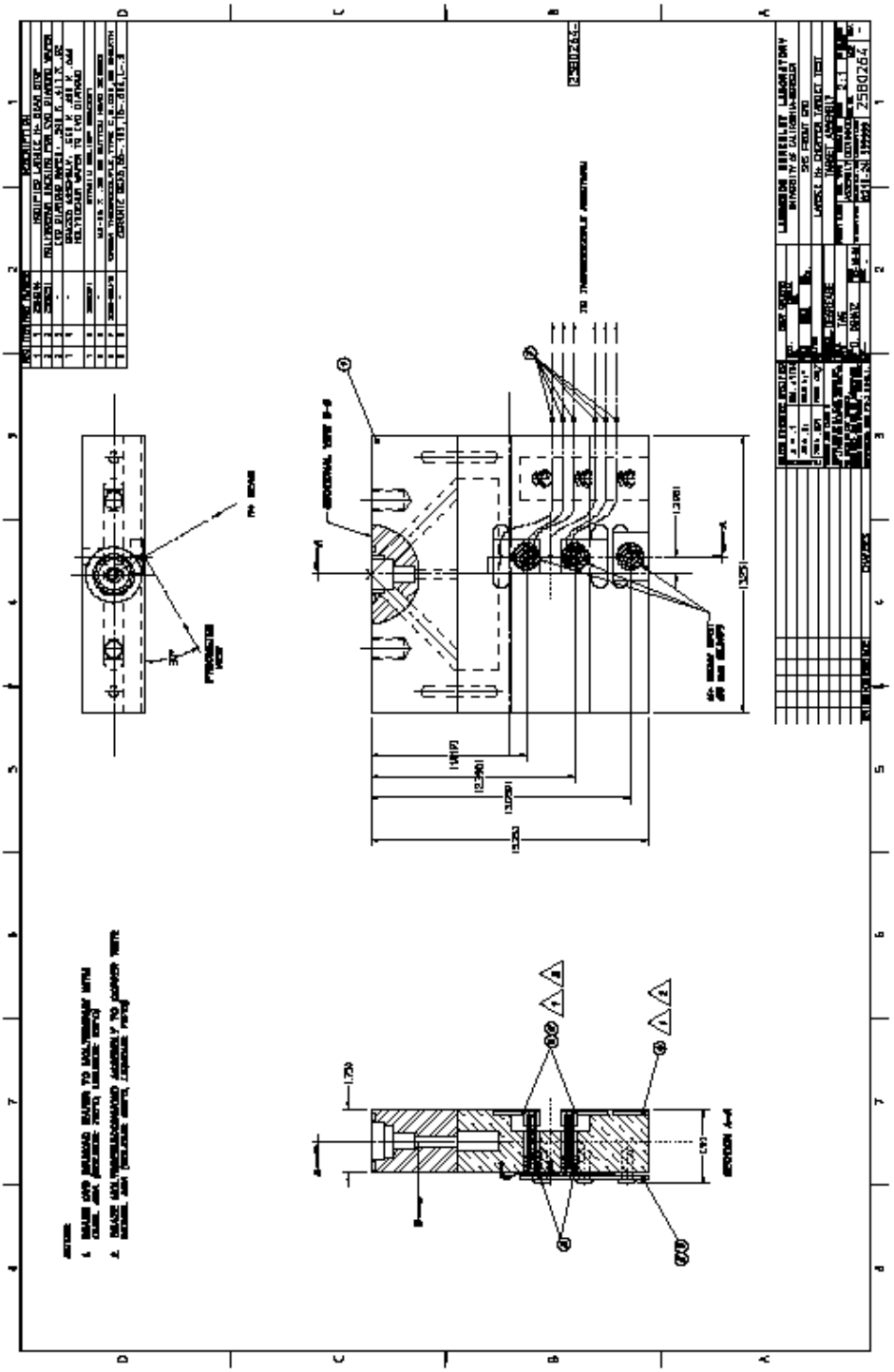

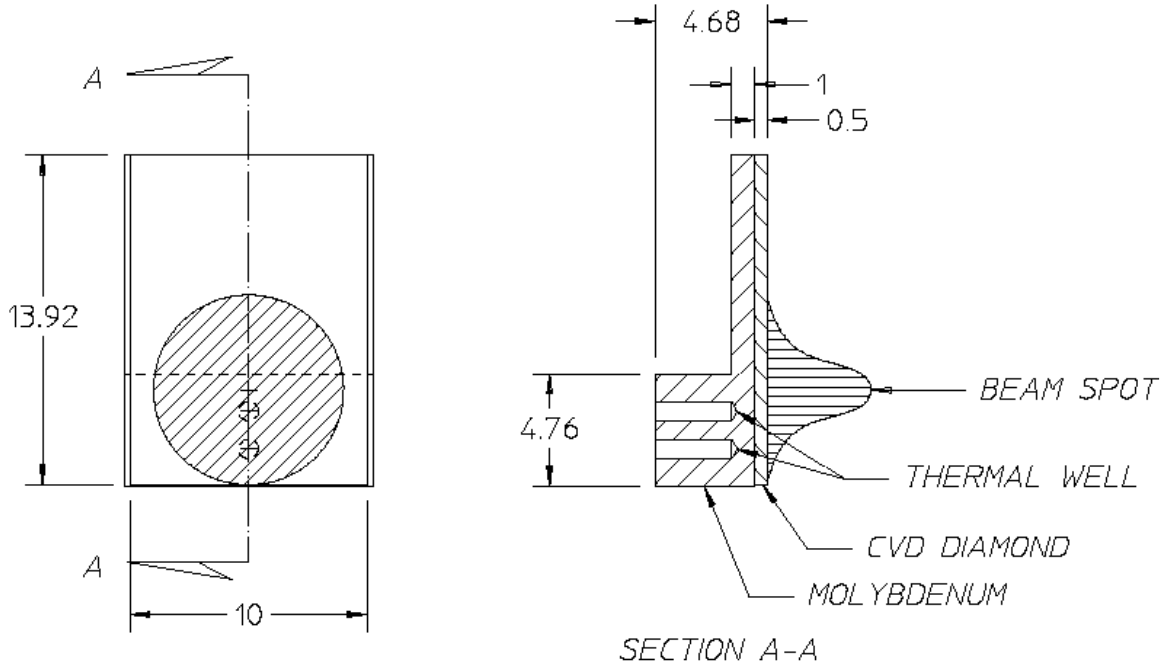

Diamond target layout

Appendix B

Pyrometer design

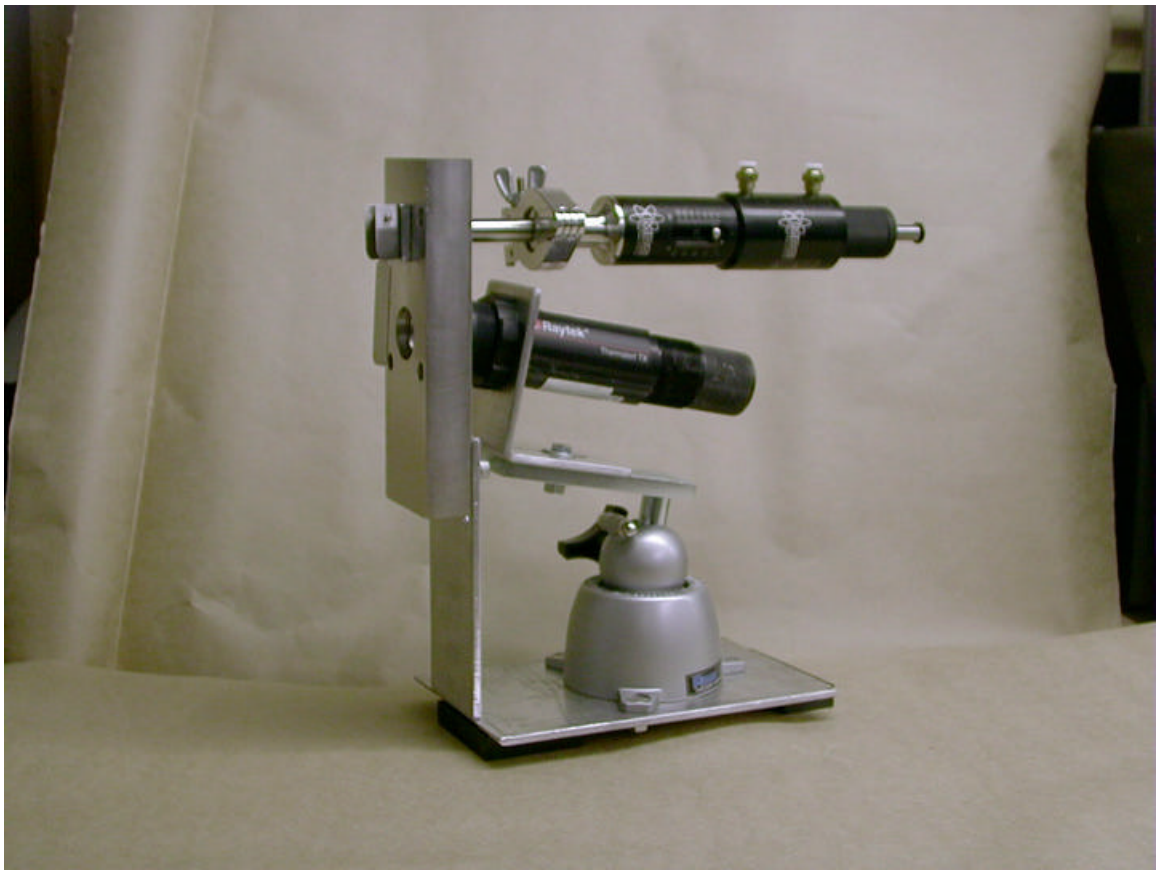

Pyrometer and hydraulic shutter on adjustable mount

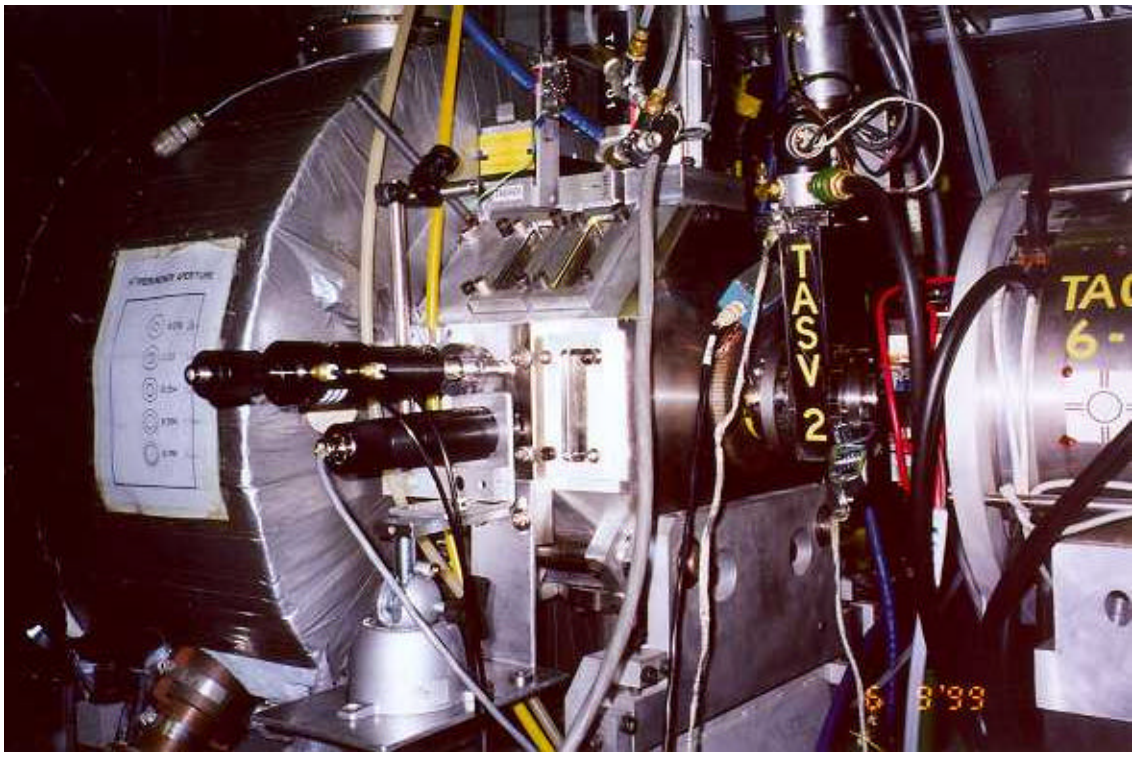

Pyrometer and shutter mounted to LANSCE beam box

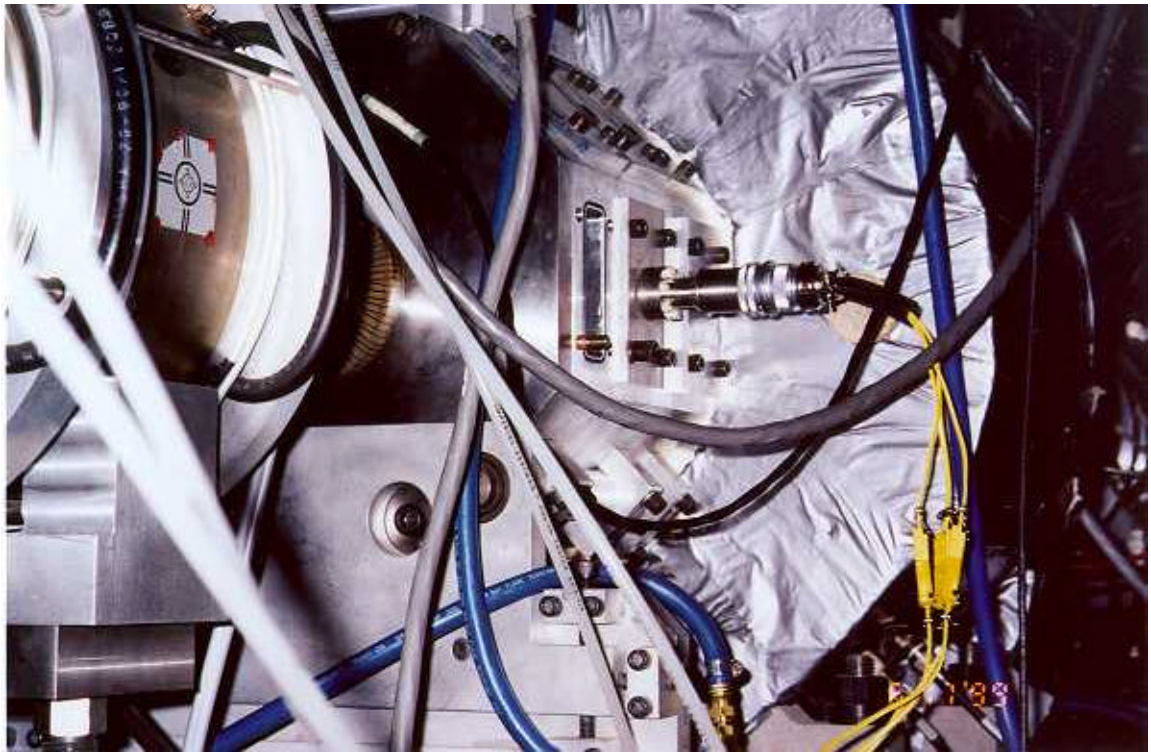
Thermocouple feedthrough mounted on LANSCE beam box

Appendix C

Emmittance Calculations

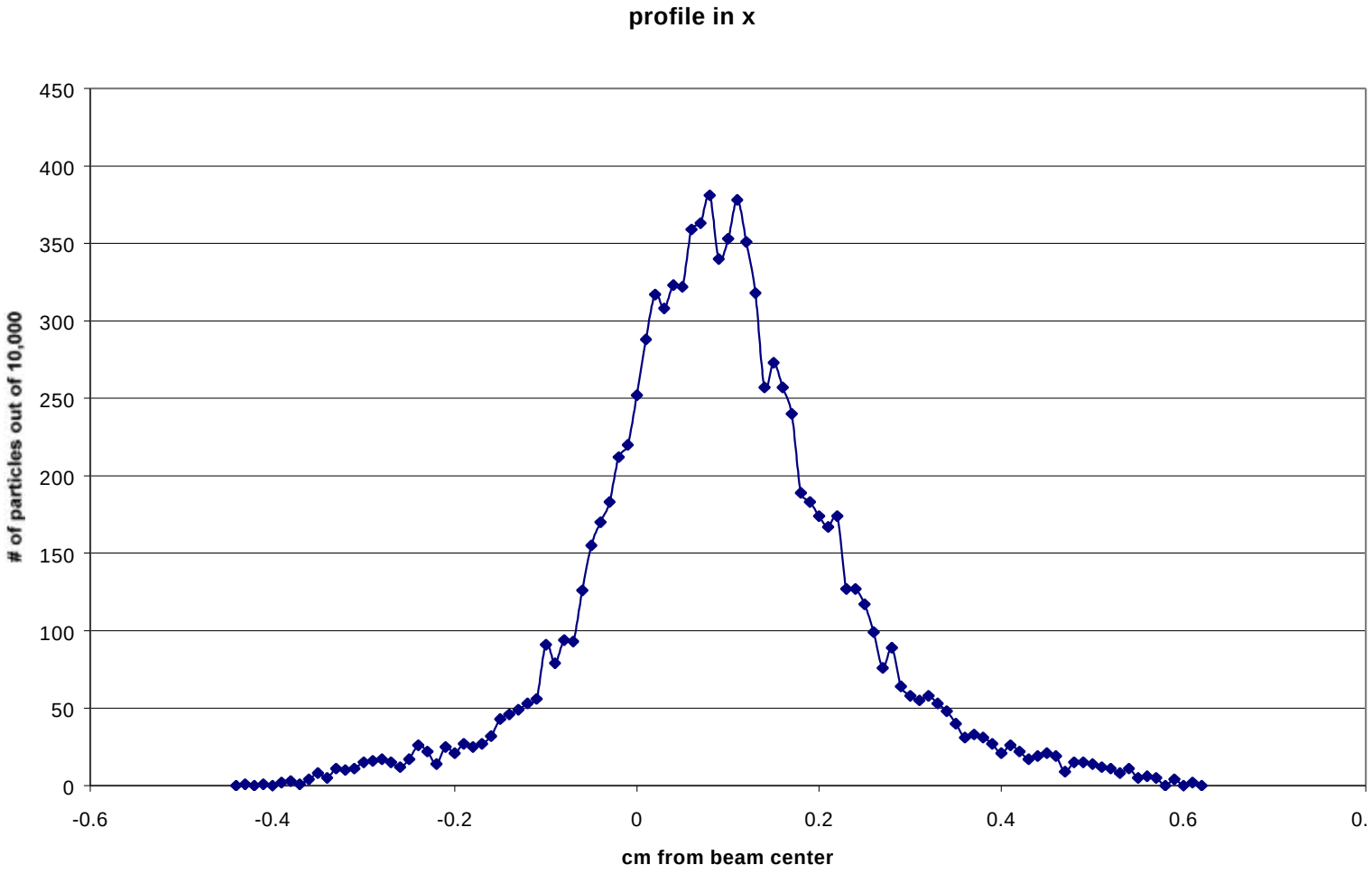

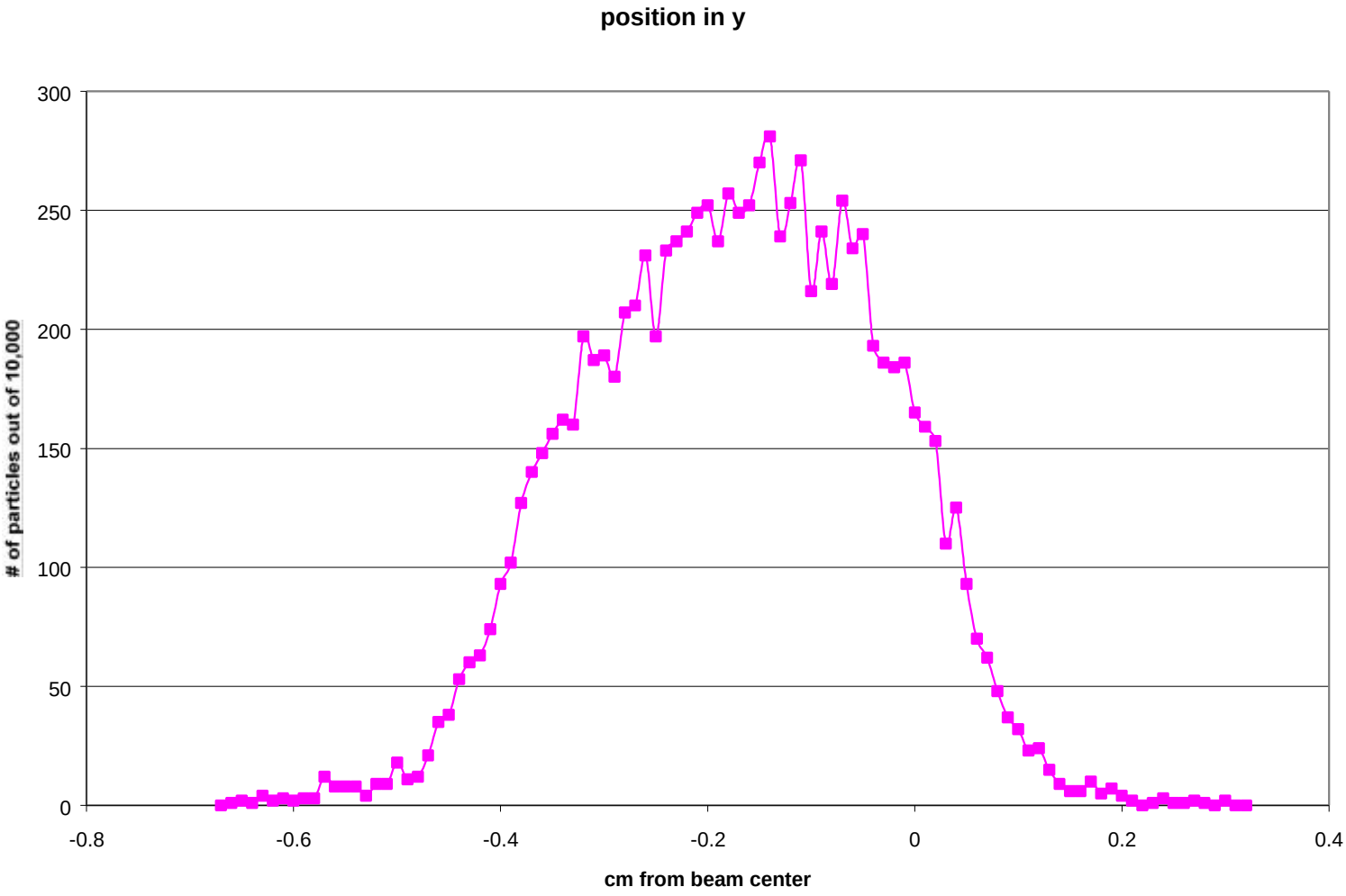
position in y
300
250
200
150
100
50
0
# of particles out of 10,000
-0.8
-0.6
-0.4
-0.2
0
0.2
0.4
cm from beam center

Appendix D

Temperature profile after applying average power across the total beam spot (6σ) to reach a steady state:

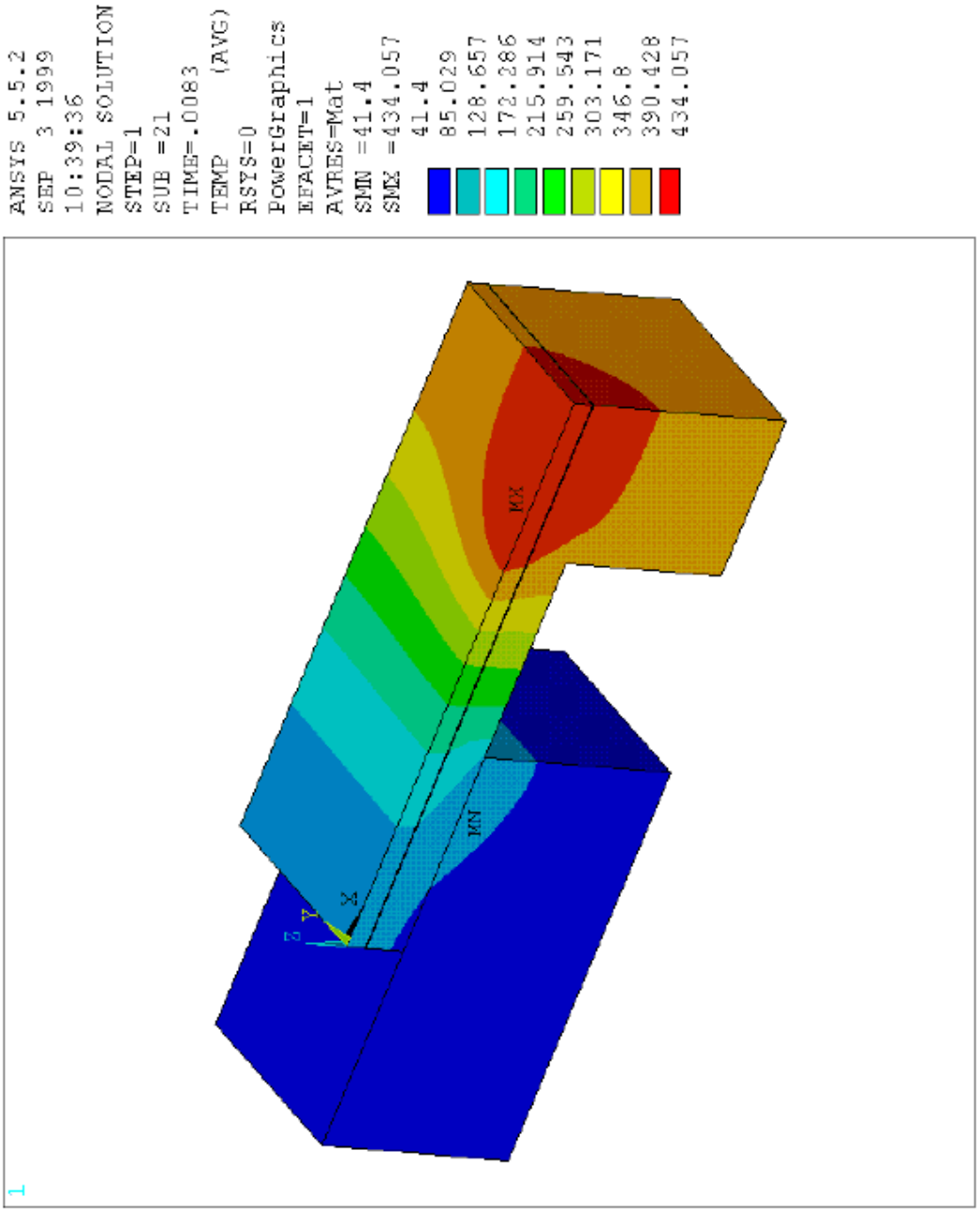

Temperature profile after initial 150 microsecond gaussian beam pulse:

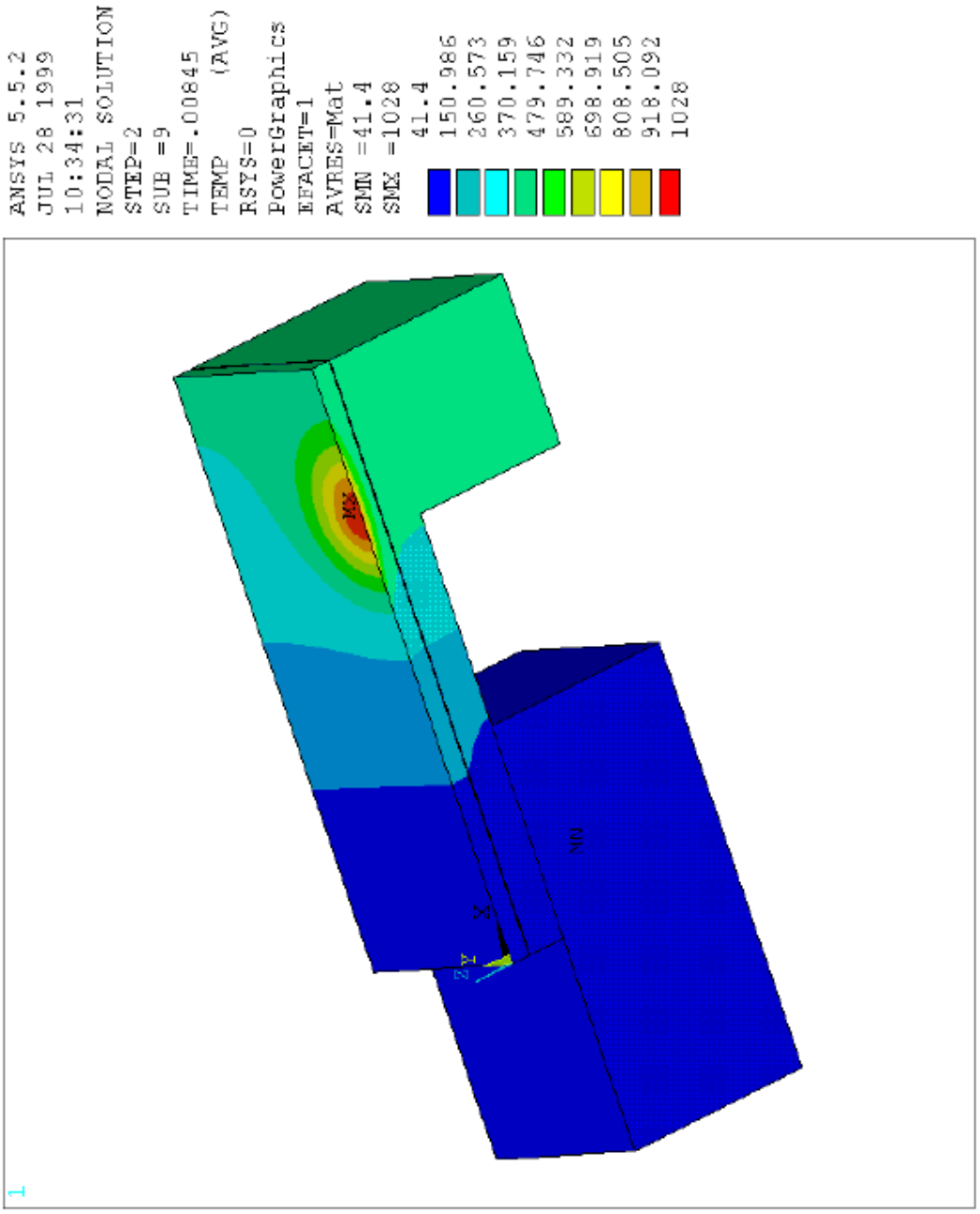

Temperature profile after cooling for 1.37 milliseconds:

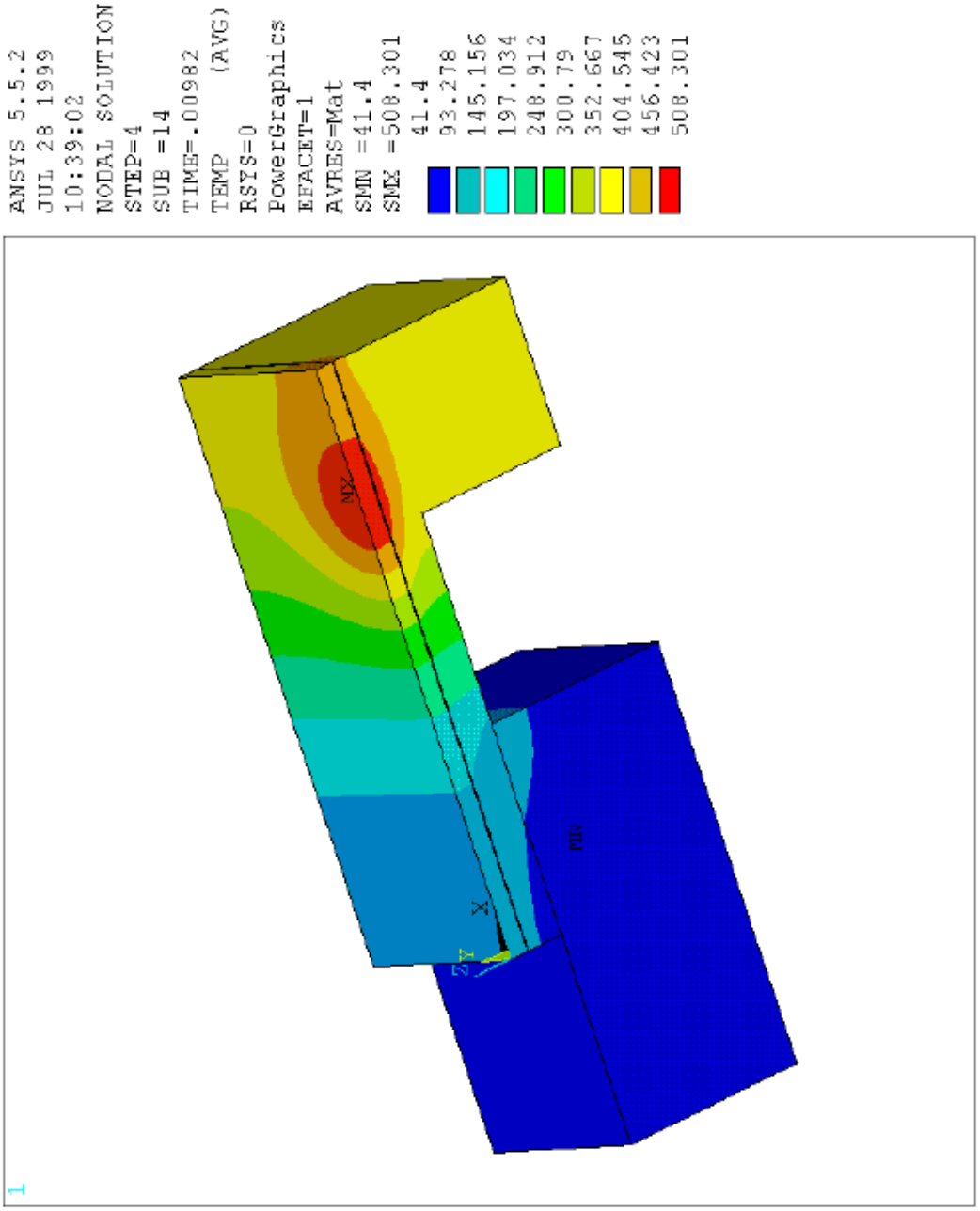

Temperature cooling after 8.15 milliseconds, immediately before arrival of next pulse:

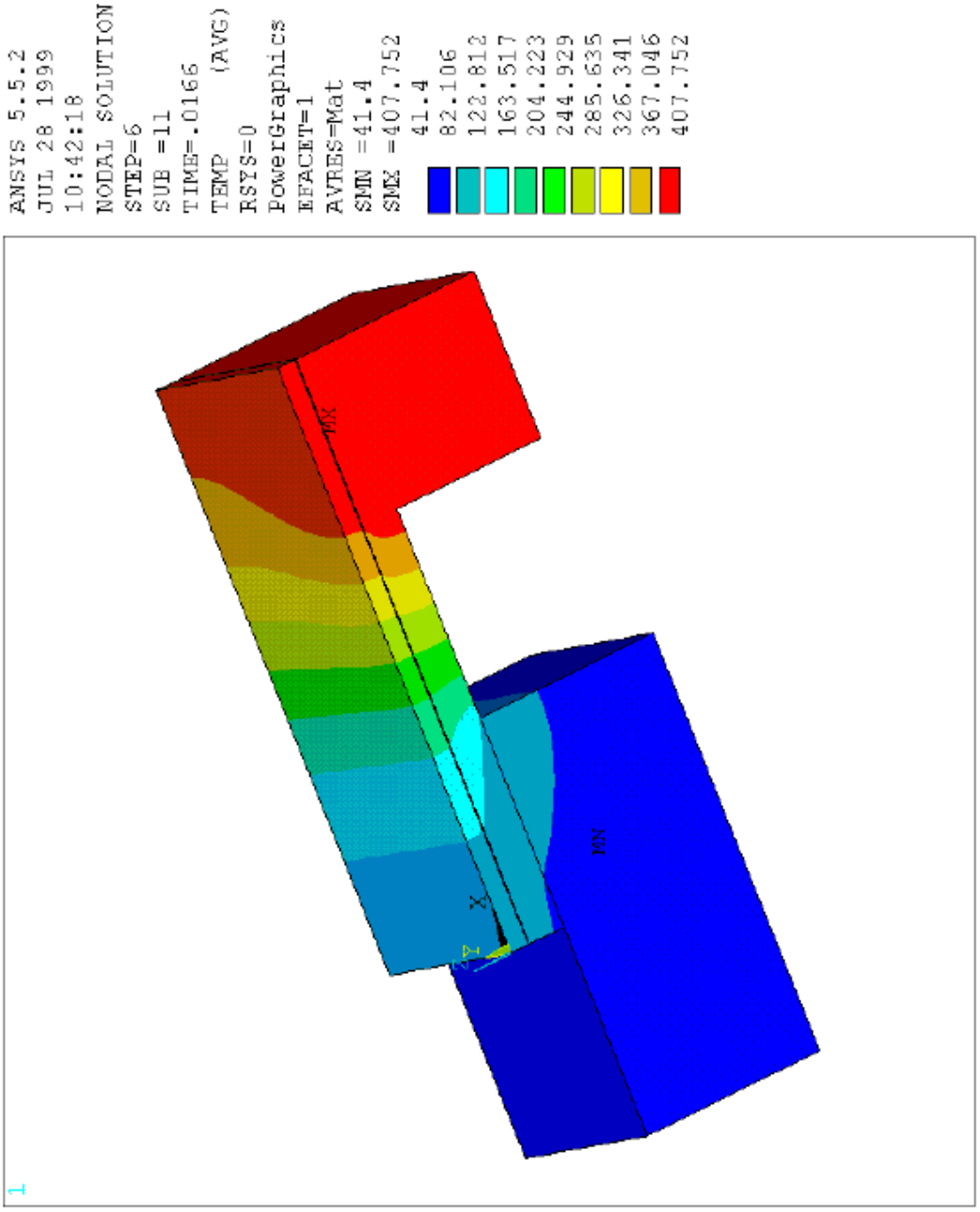

Ansys input code

```
l=14
w=10
td=-.5
tb=-.025
tm=-1
t2m=-4.17
tc=-5
lc=5
lm=10
l2m=7
l2c=-5
tdb=td+tb
tt=td+tb+tm
ttm=tt+t2m
ttc=tt+tc



ndiv=20
tempb=41.4
avgpow=270/2
sx=l2m/6
sy=l2m/6
sp=l-3*sx
r=(l-sp)/(lc)
ndivpow=ndiv*(lm-lc)/(l-sp)+ndiv*(sp-lm)/(l-sp)+ndiv
/prep7
/view,,1,1,1

k,1,0,0,0
k,2,0,w/2,0
k,3,l,w/2,0
k,4,l,0,0
k,5,lm,0,0
k,6,lm,w/2,0
k,7,lc,0,0
k,8,lc,w/2,0
k,9,l2c,0,0
k,10,l2c,w/2,0
k,11,sp,0,0
k,12,sp,w/2,0
k,13,0,0,td
k,14,0,0,tdb
k,15,0,0,tt
k,16,0,0,ttm
k,17,0,0,ttc

/auto

l,10,2     !1
l,2,8
l,8,7
l,7,1      !4
```

```
l,1,9
l,9,10
l,8,6,ndiv*(lm-lc)/(l-sp) !7
l,6,5
l,5,7,ndiv*(lm-lc)/(l-sp)
l,6,12,ndiv*(sp-lm)/(l-sp) !10
l,11,4
l,3,4
l,3,12 !13
l,11,5,ndiv*(sp-lm)/(l-sp)
l,11,12
l,2,1
lesize,all,,,ndiv

l,1,13,ndiv/4   !17
l,13,14,ndiv/ndiv
l,14,15,ndiv/4
l,15,16,ndiv/5
l,15,17,ndiv/5

al,1,16,5,6
al,16,2,3,4
al,7,8,9,3
al,10,15,14,8
al,11,12,13,15

/input,chopmat,inp,G:\Ansysdata\diamondbeam\
et,1,55
mat,1
amesh,3,5
amesh,1,2

et,2,70
type,2

!diamond layer
mat,1
vdrag,2,3,4,5,1,,17

!braze layer
asel,s,loc,z,td
mat,5
vdrag,all,,,,,18

!moly layer
asel,s,loc,z,tdb
mat,2
vdrag,all,,,,,19

!copper sink
asel,s,loc,z,tt
asel,r,loc,x,lc,l2c
mat,3
vdrag,all,,,,,21

!moly sink
```

```
asel,s,loc,z,tt
asel,r,loc,x,l,lm
mat,2
vdrag,all,,,,,20

allsel,all

/PNUM,VOLU,1

/REPLOT

!clear area nodes&elements
asel,s,loc,z,0
nsla,s,1
esln,s,1
aclear,all
alls

!clear excess volumes
vsel,s,loc,x,0,l2c
vsel,r,loc,z,0,tt
nslv,s,1
esln,s,1
vclear,all

allsel,all
/REPLOT
eplot

!apply temperature to copper sink
nsel,s,loc,z,ttc
d,all,temp,tempb
alls
nsel,s,loc,x,l2c
d,all,temp,tempb
alls

!apply constant power over spot area
!nsel,s,loc,z,0
!nsel,r,loc,x,l,l-7
!*get,nnodes,node,,count
!ppn=avgpow/nnodes
!f,all,heat,ppn
!alls

!move workplane to beamcenter
!wpoffs,l-3sx,0,0

!load steps
!antype,trans
!tuniff,tempb
!tref,tempb
!kbc,1


!bigaussian distribution to nodes-avg power to equilibrilize
```

```
nsel,s,loc,z,0
nsel,r,loc,x,lc,l
*get,nnodes,node,,count
pave=avgpow/(3.1415*sx*sy)*(l-lc)/ndivpow*w/2/ndiv
*do,cnt,1,nnodes
*get,xloc,node,cnt,loc,x
*get,yloc,node,cnt,loc,y
nsel,s,loc,z,0
nsel,r,loc,x,xloc
nsel,r,loc,y,yloc

*if,yloc,eq,0,then
f,cnt,heat,pave/2*exp(-(xloc-sp)*(xloc-sp)/(2*sx*sx)-yloc*yloc/(2*sy*sy))
*else
f,cnt,heat,pave*exp(-(xloc-sp)*(xloc-sp)/(2*sx*sx)-yloc*yloc/(2*sy*sy))
*endif
cnt=cnt+1
*enddo
alls


nsel,s,loc,z,0
nsel,r,loc,x,l-20/3*sx,lc
f,all,heat,0
alls

t=.0083
time,t
timint,off,all
lswrite,1



!bigaussian distribution to nodes total power over gate time
nsel,s,loc,z,0
nsel,r,loc,x,lc,l
*get,nnodes,node,,count
pave=avgpow*(1/.018)/(3.1415*sx*sy)*(l-lc)/ndivpow*w/2/ndiv
*do,cnt,1,nnodes
*get,xloc,node,cnt,loc,x
*get,yloc,node,cnt,loc,y
nsel,s,loc,z,0
nsel,r,loc,x,xloc
nsel,r,loc,y,yloc

*if,yloc,eq,0,then
f,cnt,heat,pave/2*exp(-(xloc-sp)*(xloc-sp)/(2*sx*sx)-yloc*yloc/(2*sy*sy))
*else
f,cnt,heat,pave*exp(-(xloc-sp)*(xloc-sp)/(2*sx*sx)-yloc*yloc/(2*sy*sy))
*endif
cnt=cnt+1
*enddo
alls
```

```
time,t+.000150
deltim,.000010,.000005,.000020
timint,on,all
autos,on
lswrite,2


!remove bigaussian distribution to nodes
nsel,s,loc,z,0
nsel,r,loc,x,lc,l
*get,nnodes,node,,count
pave=0
*do,cnt,1,nnodes
*get,xloc,node,cnt,loc,x
*get,yloc,node,cnt,loc,y
nsel,s,loc,z,0
nsel,r,loc,x,xloc
nsel,r,loc,y,yloc

*if,yloc,eq,0,then
f,cnt,heat,pave/2*exp(-(xloc-sp)*(xloc-sp)/(2*sx*sx)-yloc*yloc/(2*sy*sy))
*else
f,cnt,heat,pave*exp(-(xloc-sp)*(xloc-sp)/(2*sx*sx)-yloc*yloc/(2*sy*sy))
*endif
cnt=cnt+1
*enddo
alls


time,t+.00030
deltim,.000005,.000005,.000020
lswrite,3

time,t+.00152
deltim,.000020,.000020,.00012
lswrite,4

time,t+.00422
deltim,.00012,.00012,.00027
lswrite,5

time,t+.0083
deltim,.00027,.00027,.00041
lswrite,6
```

Material Properties Used

```
MPTEMP,1,27,127,202,500,1000              !Temp. in C

! Material #1: CVD Diamond Properties
mpdata,kxx,1,1,2.1,1.4,1.2,.6,.17     !W/mm/K
mp,c,1,516                                !J/kg/K
mp,dens,1,3.51506e-6                      !kg/mm^3
mp,ex,1,483e3                             !N/mm^2
mp,nuxy,1,.2
mp,alpx,1,3e-6                            !mm/mm/K

! Material #2: Molybdenum Properties
mpdata,kxx,2,1,.141,.137,.134,.121,.101   !W/mm/K
mpdata,c,2,1,275,275,275,275,310  !J/kg/K
mp,dens,2,9e-6                            !kg/mm^3
mp,ex,2,310e3                             !N/mm^2
mp,nuxy,2,.3
mp,alpx,2,5.4e-6                  !mm/mm/K

! Material #3: Copper / Glidcop Properties
mpdata,kxx,3,1,.398,.392,.389,.372,.335   !W/mm/K
mp,c,3,379                                !J/kg/K
mp,dens,3,8.92e-6                         !kg/mm^3
mp,ex,3,117e3                             !N/mm^2
mp,nuxy,3,.3
mp,alpx,3,16.5e-6                         !mm/mm/K

! Material #4: Titanium Properties
mp,kxx,4,.0066                            !W/mm/K
mp,c,4,580                                !J/kg/K
mp,dens,4,4.43e-6                         !kg/mm^3
mp,ex,4,116e3                             !N/mm^2
mp,nuxy,4,.3
mp,alpx,4,9e-6                            !mm/mm/K

! Material #5: Braze properties
mp,kxx,5,.18                              !W/mm/K
mp,c,5,300                                !J/kg/K GUESS???
mp,dens,5,9.8e-6                  !kg/mm^3
mp,ex,5,83e3                              !N/mm^2
mp,nuxy,5,.3
mp,alpx,5,18.5e-6                                 !mm/mm/K
```

References:

[1] Sussman, R.s., Brandon, J.R. et al., "Properties of Bulk Polycrystalline CVD Diamond" *Diamond and Related Materials*, 3 (1994) 303-312.

[2] Palmer, D.W. "Rate of production of radiation damage in diamond", *Properties and Growth of Diamond*, Davies, Gordon ed., Emis Datareviews series, 9, Inspec. 143-150.

[3] Vandersande, J.W., "Effects of radiation damage on the thermal conductivity of diamond" ", *Properties and Growth of Diamond*, Davies, Gordon ed., Emis Datareviews series, 9, Inspec. 182-184

[4] Kalish, R. "Implantation-induced damage and its annealing in diamond" *Properties and Growth of Diamond*, Davies, Gordon ed., Emis Datareviews series, 9, Inspec. 196-200.

[6] "Properties of Diamond" Harris Diamond Corporation promotional brochure, Mount Arlington, NJ